Available online at www.sciencedirect.com
ScienceDirect
Nuclear Medicine and Biology 33 (2006) 963–969
NUCLEAR MEDICINE — AND — BIOLOGY
www.elsevier.com/locate/nucmedbio

Radioiodinated VEGF to image tumor angiogenesis in a LS180 tumor xenograft model

Mitsuyoshi Yoshimoto[a,*], Seigo Kinuya[b], Atsuhiro Kawashima[c], Ryuichi Nishii[d,e], Kunihiko Yokoyama[b], Keiichi Kawai[a,e]

[a]*Division of Health Sciences, Graduate School of Medical Science, Kanazawa University, Ishikawa 920-0942, Japan*
[b]*Department of Biotracer Medicine, Graduate School of Medical Science, Kanazawa University, Ishikawa 920-8640, Japan*
[c]*Kanazawa Medical Center, Ishikawa 920-8650, Japan*
[d]*Department of Radiology, Fujimoto Hayasuzu Hospital, Miyazaki 885-0055, Japan*
[e]*Biomedical Imaging Research Center, University of Fukui, Fukui 910-1193, Japan*

Received 28 April 2006; received in revised form 9 August 2006; accepted 10 August 2006

Abstract

Introduction: Angiogenesis is essential for tumor growth or metastasis. A method involving noninvasive detection of angiogenic activity in vivo would provide diagnostic information regarding antiangiogenic therapy targeting vascular endothelial cells as well as important insight into the role of vascular endothelial growth factor (VEGF) and its receptor (flt-1 and KDR) system in tumor biology. We evaluated radioiodinated $VEGF_{121}$, which displays high binding affinity for KDR, and $VEGF_{165}$, which possesses high binding affinity for flt-1 and low affinity for KDR, as angiogenesis imaging agents using the LS180 tumor xenograft model.

Methods: $VEGF_{121}$ and $VEGF_{165}$ were labeled with ^{125}I by the chloramine-T method. Biodistribution was observed in an LS180 human colon cancer xenograft model. Additionally, autoradiographic imaging and immunohistochemical staining of tumors were performed with ^{125}I-$VEGF_{121}$.

Results: ^{125}I-$VEGF_{121}$ and ^{125}I-$VEGF_{165}$ exhibited strong, continuous uptake by tumors and the uterus, an organ characterized by angiogenesis. ^{125}I-$VEGF_{121}$ uptake in tumors was twofold higher than that of ^{125}I-$VEGF_{165}$ (9.12±98 and 4.79±1.08 %ID/g at 2 h, respectively). ^{125}I-$VEGF_{121}$ displayed higher tumor to nontumor (T/N) ratios in most normal organs in comparison with ^{125}I-$VEGF_{165}$. ^{125}I-$VEGF_{121}$ accumulation in tumors decreased with increasing tumor volume. Autoradiographic and immunohistochemical analyses confirmed that the difference in ^{125}I-$VEGF_{121}$ tumor accumulation correlated with degree of tumor vascularity.

Conclusion: Radioiodinated $VEGF_{121}$ is a promising tracer for noninvasive delineation of angiogenesis in vivo.

Keywords: Tumor imaging; Angiogenesis; VEGF; VEGF receptors

1. Introduction

Tumors require angiogenesis in order to grow beyond the size of 1–2 mm in diameter, a condition in which nutrients and oxygen are not adequately supplied via passive diffusion through existing blood vessels [1]. Furthermore, the metastatic property of tumors strongly correlates with tumor angiogenesis [2,3]. In particular, the balance between various activators and inhibitors closely associated with overexpression of vascular endothelial growth factor (VEGF) and its receptors serves to regulate angiogenesis. It is well known that VEGF plays a pivotal role in angiogenesis — proliferation and migration of endothelial cells. Five VEGF isoforms, produced by alternative splicing of responsible genes, have been identified. $VEGF_{121}$ and $VEGF_{165}$ are the predominant isoforms [4]. Endothelial cells express two VEGF receptors (VEGFRs): flt-1 (K_d=26±6 pM for $VEGF_{165}$) and KDR (K_d=80±13 pM for $VEGF_{121}$, K_d=2070±520 pM for $VEGF_{165}$) [5]. These receptors are up-regulated in endothelial cells in tumor tissue [6,7].

Numerous compounds possessing an antiangiogenic profile have been investigated [8–10]. Conventional anti-tumor agents act directly on tumor cells. In contrast, most antiangiogenic agents primarily target endothelial cells,

* Corresponding author. Tel.: +81 76 265 2539; fax: +81 76 234 4366.
E-mail address: myoshi@mhs.mp.kanazawa-u.ac.jp (M. Yoshimoto).

0969-8051/$ – see front matter © 2006 Elsevier Inc. All rights reserved.
doi:10.1016/j.nucmedbio.2006.08.006

which enables their application to various types of tumors. Most antiangiogenic agents target the VEGF–VEGFR system, which inhibits proliferation of endothelial cells [11–14].

Despite its invasive nature, conventional angiography has been the standard imaging tool for evaluation of tumor vascularity. Less invasive approaches such as computed tomographic angiography and, more recently, three-dimensional magnetic resonance angiography can effectively demonstrate the vasculature. These modalities, however, merely delineate preexisting vasculature; they do not disclose the dynamic changes in blood vessels (endothelial cells) attributable to antiangiogenic therapy. Positron emission tomography and single photon emission computed tomography may enable lesional characterization in the management of cancer patients. Positron tracers such as 2-^{18}F-fluoro-2-deoxyglucose (^{18}F-FDG) and 3′-deoxy-3′-^{18}F-fluorothymidine (^{18}F-FLT) would afford data corresponding to tumor therapeutic responses. The major action of antiangiogenic therapy is the induction of dormancy of tumors, which may alter glycolysis or DNA synthesis in tumors. However, alternations in these cellular functions in antiangiogenic therapy occur secondarily, following the primary effects of antiangiogenic agents on endothelial cells. So-called perfusion agents, e.g., ^{201}Tl, ^{99m}Tc-sestamibi and ^{99m}Tc-tetrofosmin, would also be inadequate, as factors other than tissue perfusion substantially affect the distribution of these tracers. For instance, ^{99m}Tc-sestamibi accumulation in brain tumors is independent of tumor vascularization [15]. Neo-angiogenesis in tumors is strongly correlated with patient prognosis; consequently, a method enabling noninvasive estimation of angiogenesis in vivo would surely provide beneficial clinical information. Furthermore, such information may permit selection of those patients most likely to benefit from antiangiogenic therapy as well as facilitate monitoring of its efficacy.

In order to develop noninvasive, specific techniques for estimation of tumor vascularity, this investigation utilized $VEGF_{121}$ and $VEGF_{165}$ radiolabeled with ^{125}I. The specificity and binding ability of $VEGF_{121}$ and $VEGF_{165}$ to receptors have been well established with ^{125}I-$VEGF_{121}$ and ^{125}I-$VEGF_{165}$ in biochemical field. These compounds were evaluated as candidates for angiogenesis imaging using a human cancer xenograft model.

2. Materials and methods

2.1. Radioiodination of VEGF

Radioiodination of human recombinant $VEGF_{121}$ (R&D Systems, Minneapolis, MN) and $VEGF_{165}$ (PeproTech EC, London, UK) was performed via the chloramine-T method described previously [5,16]. Briefly, 1.0 μg of $VEGF_{121}$ or $VEGF_{165}$ was labeled with approximately 18.5 MBq of Na^{125}I (Amersham Pharmacia, Buckinghamshire, UK) and 25 μg of chloramine-T in 20 mM phosphate buffer (pH 7.2) in a final volume of 110 μl. Iodination was allowed to proceed at room temperature for 1 min. The reaction was terminated upon the addition of 5 μl of sodium metabisulfite (5 mg/ml). ^{125}I-$VEGF_{121}$ and ^{125}I-$VEGF_{165}$ were purified on a gel filtration (Sephadex G-25) column (Amersham Biosciences, Uppsala, Sweden) and on a Heparin-Sepharose column (Amersham Biosciences), respectively. ^{125}I-$VEGF_{121}$ and ^{125}I-$VEGF_{165}$ displayed specific activities of 13.0–18.5 and 7.2–8.0 GBq/mg, respectively.

2.2. Cell culture

LS180 human colorectal adenocarcinoma cell line was purchased from Dai-Nippon Seiyaku Co. Ltd. (Japan) and grown in Eagle's minimal essential medium (Sigma, St. Louis, MO) containing 2 mM L-glutamine, nonessential amino acids and 10% FBS. Cells were cultured in a 5% CO_2-humidified atmosphere at 37°C.

2.3. Serum stability

Mouse serum (50 μl) was mixed with 18.5 kBq of ^{125}I-$VEGF_{121}$ and ^{125}I-$VEGF_{165}$, respectively, and was incubated at 37°C. After incubation for 0, 1, 2 and 4 h, trichloroacetic acid (TCA) was added to the samples. Precipitates were filtrated on glass filters, and the filters were washed with 5% TCA. Radioactivity in precipitates at 0 h was used as control. Percent precipitability of control was calculated.

2.4. Biodistribution of ^{125}I-VEGF

Animal studies were performed in compliance with guidelines for the care and use of laboratory animals of Kanazawa University. Biodistribution studies were conducted in nude mice bearing LS180 tumor. Balb/c *nu/nu* female mice, 5–6 weeks of age (Japan SLC, Inc., Shizuoka, Japan), were xenografted subcutaneously in the left thigh with 5×10^6 LS180 cells. LS180 displays considerable VEGF production and no VEGF receptors; moreover, this growth is suppressed by an anti-VEGF antibody in vivo [17]. Biodistribution was examined at 7, 10 and 14 days after implantation in order to include various tumor sizes. Mice were injected via the tail vein with 55.5 kBq/100 μl (saline containing 1% bovine serum albumin) ^{125}I-$VEGF_{121}$ or ^{125}I-$VEGF_{165}$. Mice were sacrificed at 0.5, 1, 2, 4 and 24 h postinjection, and tissue samples were excised. Tissue samples were weighed and radioactivity was measured with a γ-counter (ARC-1000M, Aloka, Tokyo, Japan). Uptake in

Table 1
Serum stability of ^{125}I-$VEGF_{121}$ and ^{125}I-$VEGF_{165}$ evaluated by TCA precipitability measurements

	Incubation time		
	1 h	2 h	4 h
^{125}I-$VEGF_{121}$	93.8±2.0	92.5±1.2	94.9±2.6
^{125}I-$VEGF_{165}$	97.3±2.2	96.8±0.9	97.5±0.7

The stability was expressed as the percent precipitant of control (n=2–3).

Table 2
Biodistribution of ^{125}I-VEGF$_{121}$ in LS180 tumor-bearing mice (n=4)

Organ	Time after injection				
	0.5 h	1 h	2 h	4 h	24 h
Tumor	5.94±0.41	8.43±0.58	9.12±0.98	9.02±1.59	2.55±0.28
Blood	40.32±2.45	38.69±4.34	32.03±0.59	24.90±2.99	7.19±0.57
Brain	0.88±0.13	0.89±0.17	0.70±0.08	0.44±0.03	0.16±0.02
Liver	7.16±0.62	6.86±1.15	5.49±0.44	5.21±0.57	1.44±0.11
Uterus	6.62±2.39	11.24±3.70	13.76±2.19	15.58±4.13	3.72±0.88
Heart	9.36±1.59	9.43±1.04	8.39±0.41	6.48±1.05	2.09±0.18
Lung	18.88±3.11	18.54±2.26	13.31±2.05	14.11±1.62	3.56±0.37
Stomach	4.49±0.39	7.32±0.94	8.81±1.87	10.85±2.18	4.23±1.22
Kidney	14.91±0.60	14.16±0.78	11.46±0.78	9.21±1.04	3.00±0.14
Pancreas	1.97±0.20	3.27±0.53	2.30±0.73	2.91±0.15	1.17±0.21
Spleen	6.77±0.89	6.46±0.34	5.90±1.36	4.53±0.79	1.67±0.11
Muscle	1.27±0.33	1.33±0.06	2.48±0.86	1.74±0.44	0.90±0.10
Bone	3.32±0.66	4.19±1.22	4.90±1.05	2.76±0.18	1.12±0.28
Intestine	3.40±0.69	3.93±0.74	3.84±0.36	3.10±0.19	1.08±0.13

Radioactivity in organs was expressed as %ID/g tissue (mean±S.D.).
Tumor volume used in this study was less than 200 mm^3.

organs was expressed as percent injected dose per gram (%ID/g) of tissue.

2.5. Autoradiography of ^{125}I-VEGF$_{121}$ in tumor

^{125}I-VEGF$_{121}$ displayed higher tumor to nontumor (T/N) ratio in comparison to ^{125}I-VEGF$_{165}$; as a result, intratumoral distribution of ^{125}I-VEGF$_{121}$ was analyzed autoradiographically (ARG). Mice were injected via the tail vein with 740–999 kBq/100 μl. Tumors were excised from mice at 4 h postinjection. Specimens were embedded in OCT compound (Sakura Finetechnical Co. Ltd., Tokyo, Japan) and frozen in dry ice–acetone. Frozen sections were cut to 20-μm thickness with a cryostat and mounted on glass slides. Glass slides were placed on an imaging plate (BAS-SR 2025, Fuji Photo Film Co. Ltd., Tokyo, Japan); subsequently, the exposed plate was scanned with a bio-imaging analyzer (BAS-5000, Fuji Photo Film) to detect radioactivity.

2.6. Immunohistochemistry by CD34 in tumors

Frozen sections adjacent to the ARG specimens were sliced to 5-μm thickness and mounted on silanized slides. The sections were air-dried and fixed in cold acetone for 5 min. Subsequently, sections were rinsed in PBS to remove the OCT compound. Endogenous peroxidase activity was blocked with 0.3% H_2O_2, and nonspecific binding was blocked with 10% normal rabbit serum. After washing in PBS, rat antimouse CD34 monoclonal antibody (BD pharmingen, La Jolla, CA), diluted 1:20, was applied to the sections and incubated at room temperature (RT) for 30 min. Next, after a PBS wash, biotinylated rabbit antirat IgG antibody (Vector Laboratory, Burlingame, CA), diluted 1:200, was applied to the sections and incubated at RT for 30 min. After washing again in PBS, streptavidine (Dako-Cytomation, Glostrup, Denmark), diluted 1:300, was applied to the sections, incubated at RT for 30 min, and washed again in PBS. The sections were then developed with diamino-

Table 3
Biodistribution of ^{125}I-VEGF$_{165}$ in LS180 tumor-bearing mice (n=3–5)

Organ	Time after injection				
	0.5 h	1 h	2 h	4 h	24 h
Tumor	2.06±0.40	3.09±0.72	4.79±1.08	1.84±0.08	0.17±0.03
Blood	1.88±0.25	3.33±0.46	5.15±0.55	2.48±0.45	0.61±0.52
Brain	3.17±0.22	2.53±0.14	1.88±0.51	0.76±0.06	0.31±0.01
Liver	16.15±2.05	7.71±0.23	5.72±0.95	4.26±0.05	2.58±0.31
Uterus	6.24±0.47	4.93±1.02	5.24±0.95	2.56±0.40	0.63±0.30
Heart	14.36±0.44	9.93±1.18	6.59±0.95	2.96±0.48	1.31±0.11
Lung	31.30±7.56	20.32±2.95	15.71±1.53	7.84±1.68	4.12±0.37
Stomach	12.65±1.34	17.96±6.90	32.79±10.06	23.93±8.71	1.11±0.19
Kidney	25.19±1.37	18.64±1.35	12.45±1.71	8.36±0.46	6.67±1.38
Pancreas	10.07±1.30	9.43±1.16	6.82±0.68	3.68±0.56	1.00±0.13
Spleen	17.80±2.39	9.00±1.62	6.78±1.75	4.14±0.46	2.53±0.54
Muscle	4.68±2.78	3.71±1.31	3.91±0.76	1.66±0.08	0.50±0.04
Bone	2.55±0.10	2.57±0.35	2.28±0.17	1.36±0.29	0.25±0.05
Intestine	4.13±0.16	3.87±0.74	4.15±0.36	2.53±0.51	0.43±0.05

Radioactivity in organs was expressed as %ID/g tissue (mean±S.D.).
Tumor volume used in this study was less than 220 mm^3.

benzidine (DakoCytomation) and counterstained with hematoxylin (Merck, Darmstadt, Germany). Additional slices were also examined using hematoxylin–eosin staining.

3. Results

3.1. Serum stability

Stability study showed no decrease in precipitability of ^{125}I-VEGF$_{121}$ and ^{125}I-VEGF$_{165}$ in mouse serum (Table 1). In serum, no obvious deiodination of ^{125}I-VEGF$_{121}$ and ^{125}I-VEGF$_{165}$ was found.

3.2. Biodistribution and tumor accumulation of ^{125}I-VEGF

Tables 2 and 3 summarize the results of biodistribution studies of ^{125}I-VEGF$_{121}$ and ^{125}I-VEGF$_{165}$ in LS180-bearing mice, respectively. Accumulation of ^{125}I-VEGF$_{121}$ in tumors gradually increased with time, reaching a peak (9.12 %ID/g) at 2 h postinjection; subsequently, ^{125}I-VEGF$_{121}$ accumulation remained unchanged through 4 h postinjection. The uterus demonstrated a ^{125}I-VEGF$_{121}$ accumulation pattern similar to that of tumors.

^{125}I-VEGF$_{165}$ exhibited higher accumulation in normal tissues, with the exception of blood, than ^{125}I-VEGF$_{121}$; however, ^{125}I-VEGF$_{165}$ was cleared more rapidly than ^{125}I-VEGF$_{121}$, particularly in liver, heart, lung, kidney and spleen. ^{125}I-VEGF$_{121}$ accumulation in tumors was two- and fivefold greater than that of ^{125}I-VEGF$_{165}$ at 2 and 4 h postinjection, respectively.

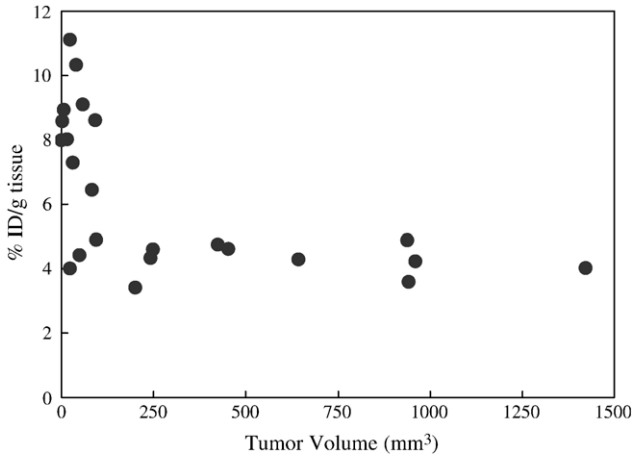

Fig. 2. Relationship between ^{125}I-VEGF$_{121}$ accumulation and tumor volume. Data correspond to ^{125}I-VEGF$_{121}$ accumulation at 4 h postinjection. LS180-xenografted mice were examined at 7, 10 and 17 days after implantation. Tumor volume was calculated as $\pi/6\times(r_1\times r_2\times r_3)$; ($r_1$: length; r_2: width; r_3: depth).

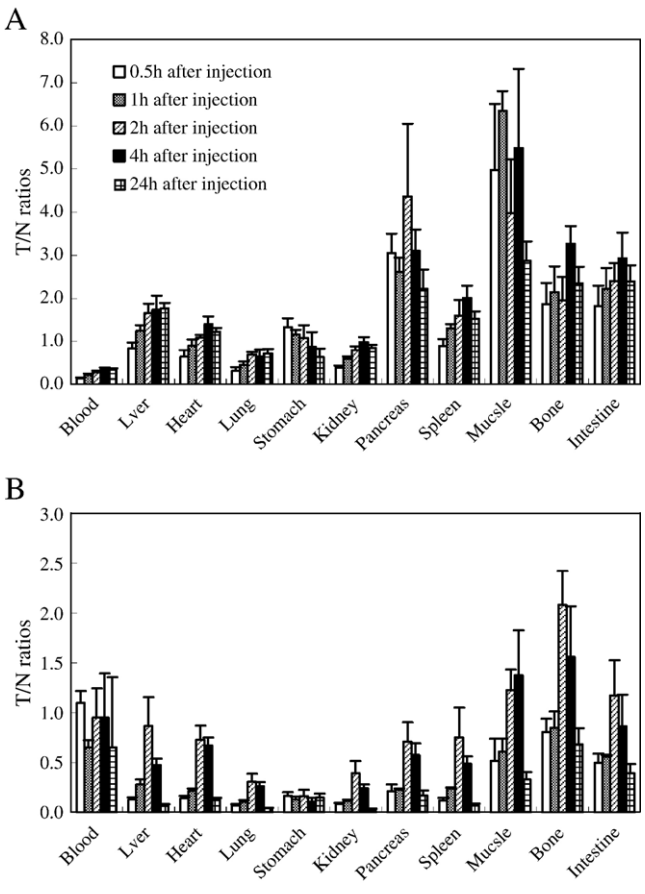

Fig. 1. Tumor to nontumor ratios in LS180 tumor-bearing mice at 0.5, 1, 2, 4 and 24 h after injection of ^{125}I-VEGF$_{121}$ (A) and ^{125}I-VEGF$_{165}$ (B). Columns, mean; bars, SD (n = 3–5).

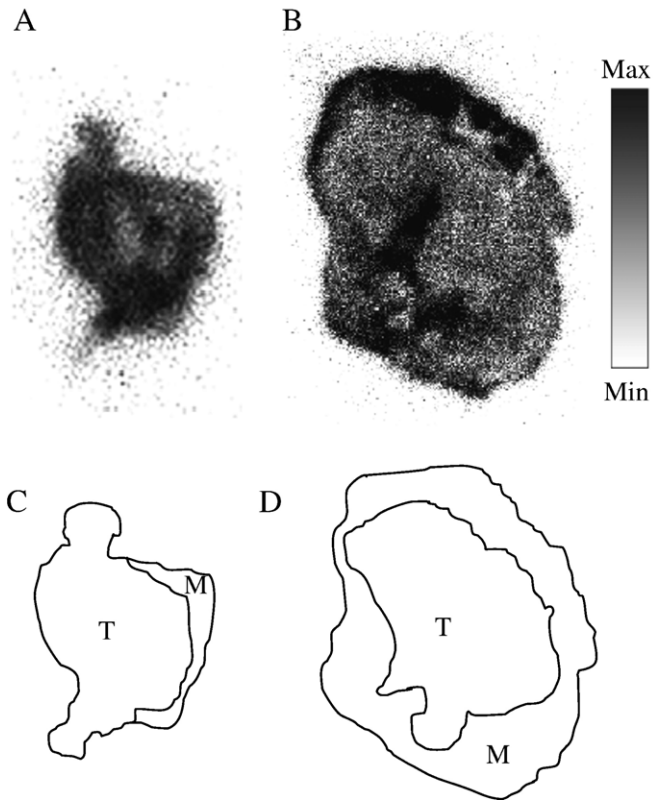

Fig. 3. Autoradiography image of intratumoral distribution at 4 h postinjection of ^{125}I-VEGF$_{121}$. Images were obtained from LS180 tumor tissues displaying volumes of (A) 101.9 mm^3 and (B) 361.9 mm$_3$. Tissue slice photos (C) and (D) correspond to ARG images (A) and (B), respectively (T: tumor; M: muscle).

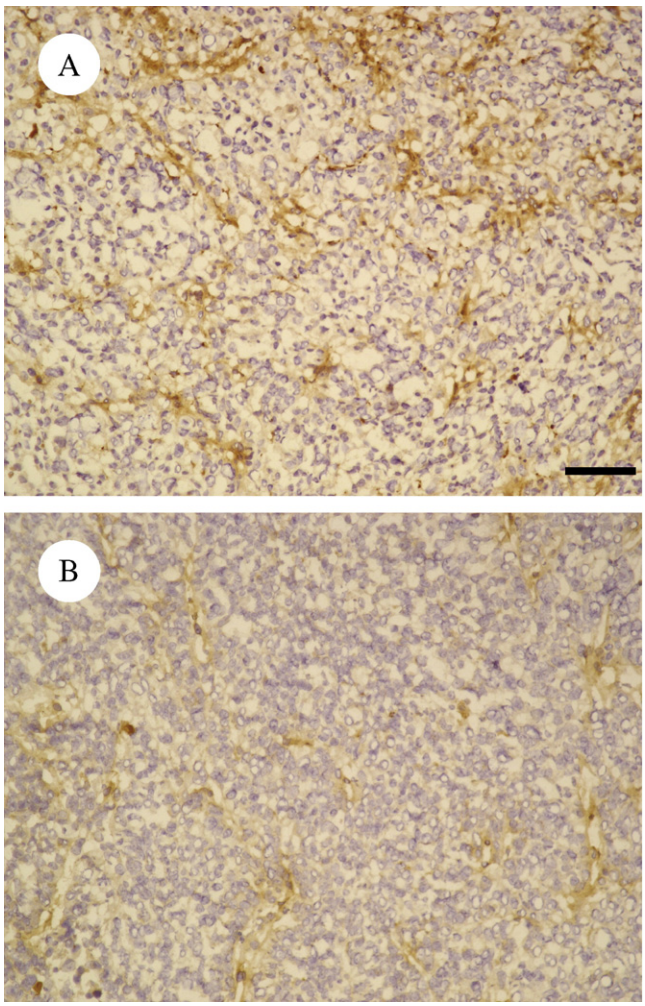

Fig. 4. Vascular staining with an anti-CD34 mAb in LS180 tumor. Images (A) and (B) are representative areas of Fig. 3A and B, respectively. Bar indicates 100 ìm in (A).

Fig. 1A and B displays T/N ratios of ^{125}I-VEGF$_{121}$ and ^{125}I-VEGF$_{165}$, respectively. Tumor-to-nontumor ratios of ^{125}I-VEGF$_{121}$ were markedly higher than those of ^{125}I-VEGF$_{165}$, with the exception of blood. Tumor-to-blood ratio of ^{125}I-VEGF$_{121}$ increased to 4 h postinjection, although the ratio was strikingly low. In contrast, the tumor-to-blood ratio of ^{125}I-VEGF$_{165}$ was maximal at 30 min; subsequently, it decreased with time.

3.3. Relationship between tumor volume and ^{125}I-VEGF121 accumulation in tumors

Fig. 2 illustrates the relationship between tumor volume (mm^3) and accumulation in tumors. ^{125}I-VEGF$_{121}$ exhibited a tendency toward diminishing accumulation in tumor with increasing tumor volume.

3.4. Autoradiography and histopathological findings

Fig. 3 displays intratumoral distribution of ^{125}I-VEGF$_{121}$. ^{125}I-VEGF$_{121}$ demonstrated overall high localization in small tumors (101.9 mm^3) (Fig. 3A). As shown in Fig. 3B, high localization of ^{125}I-VEGF$_{121}$ was evident in portions of the muscle area in large tumors (361.9 mm^3). Fibrosis was induced at regions of high ^{125}I-VEGF$_{121}$ localization in tumoral area. Homogeneous accumulation of ^{125}I-VEGF$_{121}$ was observed in the tumor area, with the exception of areas of fibrosis.

Fig. 4A and B indicates microvessel staining of tumor tissues by CD34 in Fig. 3A and B, respectively. As shown in Fig. 4A, abundant vasculature was observed in small tumors. On the other hand, poor vasculature was apparent in large tumors (Fig. 4B).

4. Discussion

Neo-angiogenesis is a common characteristic of all proliferating and metastatic tumors. Development of novel drugs possessing anti-angiogenic profile is a major area of interest in clinical oncology. In vivo detection of angiogenesis clearly affords valuable information in terms of monitoring the efficacy of anti-angiogenic therapy. The VEGF–VEGFR system would be the most suitable imaging target for this purpose as this system plays a key role in angiogenesis in tumors. Positron-labeled monoclonal antibody (VG76e) that binds human VEGF has been developed in order to measure VEGF expression in tumor tissues [18]. However, substances for imaging VEGFR density would be required to monitor therapeutic responses to anti-angiogenic agents given that most agents act as inhibitors of VEGFR. Our findings provide a rationale for VEGFR imaging in tumors utilizing radiolabeled VEGF.

^{125}I-VEGF$_{121}$ and ^{125}I-VEGF$_{165}$ displayed similarities and differences in terms of in vivo behavior in tumor-xenografted mice. High initial uptake was observed in the lung and heart, probably due to abundant vascularity in these organs. Based on the molecular sizes, ^{125}I-VEGF$_{121}$ and ^{125}I-VEGF$_{165}$ were filtered by the kidney, resulting in early large accumulation in that tissue. In addition, radioiodinated metabolites may also contribute to the accumulation in kidney. In contrast, prominent ^{125}I-VEGF$_{165}$ accumulation in the stomach in comparison to ^{125}I-VEGF$_{121}$ suggests that the former was more prone to deiodination than the latter. Furthermore, differences in tissue distribution between these two compounds were observed in various other organs, including the brain and spleen, which was likely attributable to the difference corresponding to binding sites recognized by each tracer: VEGF$_{121}$ binds only to KDR with high affinity [5,19], whereas VEGF$_{165}$ binds to flt-1 with higher affinity but possesses lower affinity for KDR [5,20]. KDR mRNA is primarily expressed in the kidney, heart, spleen and lung [21], whereas flt-1 mRNA is expressed in the brain, heart, liver, kidney and lung [22]. In kidney, heart and lung, which express both VEGFRs, ^{125}I-VEGF$_{165}$ uptake was greater than that of ^{125}I-VEGF$_{121}$. Although the precise reasons regarding the different accumulation in these organs remain unclear, previous reports have suggested a possible mechanism for this

phenomenon: the difference in the expression between flt-1 and KDR on endothelial cells in adult tissues. That is, endothelial cells in adult tissues express flt-1 mRNA in a manner similar to those in embryonic tissues [23], whereas KDR is down-regulated on endothelial cells in adult tissues relative to corresponding cells in fetal tissues [24]. These findings indicate that $VEGF_{121}$ would be the more appropriate targeting molecule of VEGFRs in terms of low background activities.

The superiority of ^{125}I-$VEGF_{121}$ was also suggested by its greater tumor accumulation as compared to ^{125}I-$VEGF_{165}$. We cannot exclude the possibility that the radioactivity in blood contributes to the radioactivity in tumor especially at early time points. However, the fact that tumor-to-blood ratios gradually increased through 4 h affords evidence of specific binding to KDR. Similarity of uptake profile of ^{125}I-$VEGF_{121}$ in tumor to that of the uterus where angiogenesis occurs physiologically also indicated its specific uptake by the receptors. Therefore, the difference in expression amount and/or binding affinity between flt-1 and KDR is an essential factor with respect to determination of targeting level in tumors between ^{125}I-$VEGF_{121}$ and ^{125}I-$VEGF_{165}$. In addition, the up-regulation of VEGFRs may affect the binding affinity of ^{125}I-$VEGF_{121}$ to flt-1 [25], resulting in high accumulation of ^{125}I-$VEGF_{121}$ in tumors.

In the clinical setting, ^{123}I-$VEGF_{165}$ scintigraphy has successfully delineated gastrointestinal tumors and their metastases in lung and liver despite the high background activity in these organs [26]. Our present results suggest that ^{123}I-$VEGF_{121}$ would lead to improved detection ability in terms of abdominal lesions relative to ^{123}I-$VEGF_{165}$ consequent to higher T/N ratios expected with ^{125}I-$VEGF_{121}$.

^{125}I-$VEGF_{121}$ uptake is greater in tumors characterized by abundant vascularity than in tumors displaying poor vascularity. Greater expression of KDR in metastatic tumors with larger vessel counts in comparison to nonmetastatic tumors with smaller vessel counts has been documented [27]. Although we could not accurately measure microvessel density due to the well-developed nature of the sinusoidal vascular network in this experimental tumor model, this previous report supports our findings.

Microvessel density is correlated with invasion and metastasis, which suggests that this parameter may serve as a powerful prognostic marker [2,3]. In addition, antiangiogenic therapy leads to diminished microvessel density [11,28]. Therefore, radioiodinated VEGF may be useful for tumor diagnosis and monitoring of anti-angiogenic therapy.

Angiostatin and endostatin are endogenous angiogenesis inhibitors and are specific inhibitors of endothelial cell proliferation. The potential of $^{123/125}$I-angiostatin and ^{99m}Tc-EC-endostatin as markers for evaluating angiogenic activity has been demonstrated [29,30]. tumor-to-nontumor ratios for liver and muscle, which are comparable, are even higher for ^{125}I-$VEGF_{121}$ in comparison with these compounds: the ratio of tumor to liver and muscle is 1.74 and 5.49 for ^{125}I-$VEGF_{121}$, 0.69 and 3.54 for $^{123/125}$I-angiostatin and 0.16 and 6.1 for ^{99m}Tc-EC-endostatin, respectively. Moreover, ^{125}I-$VEGF_{121}$ produced a higher tumor-to-intestine ratio of 2.92 relative to that of $^{123/125}$I-angiostatin and ^{99m}Tc-EC-endostatin. These findings are suggestive of the feasibility of radioiodinated $VEGF_{121}$ as a targeting agent.

A possible critical problem associated with radioiodinated $VEGF_{121}$ involves prolonged elevated radioactivity in the circulation. A plausible explanation for this phenomenon corresponds to the binding of $VEGF_{121}$ to endothelial progenitor cells and/or KDR-positive cells in the circulation. Endothelial progenitor cells that express KDR originate in the bone marrow and circulate to tissues where these cells contribute to angiogenesis [31,32]. This obstacle may be overcome by co-injection of unlabeled $VEGF_{121}$, which would suppress binding of radioiodinated $VEGF_{121}$ to KDR, leading to increased availability of free radioiodinated $VEGF_{121}$; thus, accumulation of radioiodinated $VEGF_{121}$ in tumors would be enhanced in a manner similar to that observed with ^{125}I-insuline-like growth factor (IGF)-I binding to IGF-binding proteins [33].

5. Conclusion

Diagnosis of angiogenic activity in tumors provides beneficial information concerning the efficacy of anti-angiogenic therapy and risk of distant metastasis. In this report, we confirmed that radioiodinated $VEGF_{121}$ is a promising tracer for this purpose. In terms of VEGFRs, KDR is a superior target in comparison to flt-1.

Acknowledgment

This study was supported by a Grant-in-Aid for Young Scientists (B) [KAKENHI (15790657)] from the Ministry of Education, Culture, Sports, Science and Technology, Japan.

References

[1] Folkman J. The role of angiogenesis in tumor growth. Semin Cancer Biol 1992;3:65–71.
[2] Weidner N, Semple JP, Welch WR, Folkman J. Tumor angiogenesis and metastasis — correlation in invasive breast carcinoma. N Engl J Med 1991;324:1–8.
[3] Weidner N, Carroll PR, Flax J, Blumenfeld W, Folkman J. Tumor angiogenesis correlates with metastasis in invasive prostate carcinoma. Am J Pathol 1993;143:401–9.
[4] Ferrara N, Houck K, Jakeman L, Leung DW. Molecular and biological properties of the vascular endothelial growth factor family of proteins. Endocr Rev 1992;13:18–32.
[5] Li S, Peck-Radosavljevic M, Koller E, Koller F, Kaserer K, Kreil A, et al. Characterization of ^{123}I-vascular endothelial growth factor-binding sites expressed on human tumour cells: possible implication for tumour scintigraphy. Int J Cancer 2001;91:789–96.
[6] Plate KH, Breier G, Weich HA, Risau W. Vascular endothelial growth factor is a potential tumour angiogenesis factor in human gliomas in vivo. Nature 1992;359:845–8.

[7] Plate KH, Breier G, Weich HA, Mennel HD, Risau W. Vascular endothelial growth factor and glioma angiogenesis: coordinate induction of VEGF receptors, distribution of VEGF protein and possible in vivo regulatory mechanisms. Int J Cancer 1994;59:520–9.
[8] McMahon G. VEGF receptor signaling in tumor angiogenesis. Oncologist 2000;5(Suppl 1):3–10.
[9] Los M, Voest EE. The potential role of antivascular therapy in the adjuvant and neoadjuvant treatment of cancer. Semin Oncol 2001; 28:93–105.
[10] Cross MJ, Claesson-Welsh L. FGF and VEGF function in angiogenesis: signalling pathways, biological responses and therapeutic inhibition. Trends Pharmacol Sci 2001;22:201–7.
[11] Prewett M, Huber J, Li Y, Santiago A, O'Connor W, King K, et al. Antivascular endothelial growth factor receptor (fetal liver kinase 1) monoclonal antibody inhibits tumor angiogenesis and growth of several mouse and human tumors. Cancer Res 1999;59:5209–18.
[12] Gangjee A, Yang J, Ihnat MA, Kamat S. Antiangiogenic and antitumor agents: design, synthesis, and evaluation of novel 2-amino-4-(3-bromoanilino)-6-benzylsubstituted pyrrolo[2,3-*d*]pyrimidines as inhibitors of receptor tyrosine kinases. Bioorg Med Chem 2003;11:5155–70.
[13] Furet P, Bold G, Hofmann F, Manley P, Meyer T, Altmann KH. Identification of a new chemical class of potent angiogenesis inhibitors based on conformational considerations and database searching. Bioorg Med Chem Lett 2003;13:2967–71.
[14] Ueda Y, Yamagishi T, Samata K, Ikeya H, Hirayama N, Takashima H, et al. A novel low molecular weight antagonist of vascular endothelial growth factor receptor binding: VGA1155. Mol Cancer Ther 2003; 2:1105–11.
[15] Staudenherz A, Wolfsberger S, Killer M, Nasel C, Puig S, Marosi C, et al. Microvessel density is not crucial for scintigraphic visualization of brain tumors using ^{99m}Tc-MIBI. Microvasc Res 2004;67: 218–22.
[16] Cooper ME, Vranes D, Youssef S, Stacker SA, Cox AJ, Rizkalla B, et al. Increased renal expression of vascular endothelial growth factor (VEGF) and its receptor VEGFR-2 in experimental diabetes. Diabetes 1999;48:2229–39.
[17] Asano M, Yukita A, Suzuki H. Wide spectrum of antitumor activity of a neutralizing monoclonal antibody to human vascular endothelial growth factor. Jpn J Cancer Res 1999;90:93–100.
[18] Collingridge DR, Carroll VA, Glaser M, Aboagye EO, Osman S, Hutchinson OC, et al. The development of [^{124}I]iodinated-VG76e: a novel tracer for imaging vascular endothelial growth factor in vivo using positron emission tomography. Cancer Res 2002;62:5912–9.
[19] Gitay-Goren H, Cohen T, Tessler S, Soker S, Gengrinovitch S, Rockwell P, et al. Selective binding of $VEGF_{121}$ to one of the three vascular endothelial growth factor receptors of vascular endothelial cells. J Biol Chem 1996;271:5519–23.
[20] Waltenberger J, Claesson-Welsh L, Siegbahn A, Shibuya M, Heldin CH. Different signal transduction properties of KDR and Flt1, two receptors for vascular endothelial growth factor. J Biol Chem 1994;269:26988–95.
[21] Matthews W, Jordan CT, Gavin M, Jenkins NA, Copeland NG, Lemischka IR. A receptor tyrosine kinase cDNA isolated from a population of enriched primitive hematopoietic cells and exhibiting close genetic linkage to c-kit. Proc Natl Acad Sci U S A 1991; 88:9026–30.
[22] Shibuya M, Yamaguchi S, Yamane A, Ikeda T, Tojo A, Matsushime H, et al. Nucleotide sequence and expression of a novel human receptor-type tyrosine kinase gene (*flt*) closely related to the *fms* family. Oncogene 1990;5:519–24.
[23] Peters KG, De Vries C, Williams LT. Vascular endothelial growth factor receptor expression during embryogenesis and tissue repair suggests a role in endothelial differentiation and blood vessel growth. Proc Natl Acad Sci U S A 1993;90:8915–9.
[24] Millauer B, Wizigmann-Voos S, Schnürch H, Martinez R, Møller NP, Risau W, et al. High affinity VEGF binding and developmental expression suggest Flk-1 as a major regulator of vasculogenesis and angiogenesis. Cell 1993;72:835–46.
[25] Eckelman EC, Mathis CA. Targeting proteins in vivo: in vitro guidelines. Nucl Med Biol 2006;33:161–4.
[26] Li S, Peck-Radosavljevic M, Kienast O, Preitfellner J, Hamilton G, Kurtaran A, et al. Imaging gastrointestinal tumours using vascular endothelial growth factor-165 ($VEGF_{165}$) receptor scintigraphy. Ann Oncol 2003;14:1274–7.
[27] Takahashi Y, Kitadai Y, Bucana CD, Cleary KR, Ellis LM. Expression of vascular endothelial growth factor and its receptor, KDR, correlates with vascularity, metastasis, and proliferation of human colon cancer. Cancer Res 1995;55:3964–8.
[28] Laird AD, Christensen JG, Li G, Carver J, Smith K, Xin X, et al. SU6668 inhibits Flk-1/KDR and PDGFβ in vivo, resulting in rapid apoptosis of tumor vasculature and tumor regression in mice. FASEB J 2002;16:681–90.
[29] Yang DJ, Kim KD, Schechter NR, Yu DF, Wu P, Azhdarinia A, et al. Assessment of antiangiogenic effect using ^{99m}Tc-EC-endostatin. Cancer Biother Radiopharm 2002;17:233–45.
[30] Lee KH, Song SH, Paik JY, Byun SS, Lee SY, Choe YS, et al. Specific endothelial binding and tumor uptake of radiolabeled angiostatin. Eur J Nucl Med Mol Imaging 2003;30:1032–7.
[31] Asahara T, Murohara T, Sullivan A, Silver M, van der Zee R, Li T, et al. Isolation of putative progenitor endothelial cells for angiogenesis. Science 1997;275:964–7.
[32] Asahara T, Masuda H, Takahashi T, Kalka C, Pastore C, Silver M, et al. Bone marrow origin of endothelial progenitor cells responsible for postnatal vasculogenesis in physiological and pathological neovascularization. Circ Res 1999;85:221–8.
[33] Sun BF, Kobayashi H, Le N, Yoo TM, Drumm D, Paik CH, et al. Effects of insulinlike growth factor binding proteins on insulinlike growth factor-I biodistribution in tumor-bearing nude mice. J Nucl Med 2000;41:318–26.